

Accepted Manuscript

Paleozoic accretionary orogenesis in the eastern Beishan orogen: Constraints from zircon U-Pb and $^{40}\text{Ar}/^{39}\text{Ar}$ geochronology

Songjian Ao, Wenjiao Xiao, Brian F. Windley, Qigui Mao, Chunming Han, Ji'en Zhang, Liekun Yang, Jianzhen Geng

PII: S1342-937X(15)00089-1
DOI: doi: [10.1016/j.gr.2015.03.004](https://doi.org/10.1016/j.gr.2015.03.004)
Reference: GR 1424

To appear in: *Gondwana Research*

Received date: 28 November 2014
Revised date: 3 March 2015
Accepted date: 3 March 2015



Please cite this article as: Ao, Songjian, Xiao, Wenjiao, Windley, Brian F., Mao, Qigui, Han, Chunming, Zhang, Ji'en, Yang, Liekun, Geng, Jianzhen, Paleozoic accretionary orogenesis in the eastern Beishan orogen: Constraints from zircon U-Pb and $^{40}\text{Ar}/^{39}\text{Ar}$ geochronology, *Gondwana Research* (2015), doi: [10.1016/j.gr.2015.03.004](https://doi.org/10.1016/j.gr.2015.03.004)

This is a PDF file of an unedited manuscript that has been accepted for publication. As a service to our customers we are providing this early version of the manuscript. The manuscript will undergo copyediting, typesetting, and review of the resulting proof before it is published in its final form. Please note that during the production process errors may be discovered which could affect the content, and all legal disclaimers that apply to the journal pertain.

**Paleozoic accretionary orogenesis in the eastern Beishan
orogen: constraints from zircon U-Pb and $^{40}\text{Ar}/^{39}\text{Ar}$
geochronology**

Songjian Ao^{1,*}, Wenjiao Xiao^{1,2,3}, Brian F. Windley³, Qigui Mao³, Chunming Han¹,
Ji'en Zhang¹, Liekun Yang¹, Jianzhen Geng⁶,

1. *State Key Laboratory of Lithospheric Evolution, Institute of Geology and Geophysics, Chinese Academy of Sciences, Beijing 100029, China*
2. *Xinjiang Research Center for Mineral Resources, Xinjiang Institute of Ecology and Geography, Chinese Academy of Sciences, Urumqi 830011, P.R. China*
3. *CAS Center for Excellence in Tibetan Plateau Earth Sciences, China*
4. *Department of Geology, University of Leicester, Leicester LE1 7RH, UK*
5. *Beijing Institute of Geology for Mineral Resources, Beijing 100012, China*
6. *Tianjin Institute of Geology and Mineral Resources, Tianjin 300170, China*

*Corresponding author: Songjian Ao

Fax: +86 10 6201 0846; E-mail: asj@mail.igcas.ac.cn

Manuscript submitted to Special Issue in

Gondwana Research

April 16, 2015

Abstract

The continental growth mechanism of the Altaids in Central Asia is still in controversy between models of continuous subduction-accretion *versus* punctuated accretion by closure of multiple oceanic basins. The Beishan orogenic belt, located in the southern Altaids, is a natural laboratory to address this controversy. Key questions that are heavily debated are: the closure time and subduction polarity of former oceans, the emplacement time of ophiolites, and the styles of accretion and collision. This paper reports new structural data, zircon ages and Ar-Ar dates from the eastern Beishan Orogen that provide information on the accretion process and tectonic affiliation of various terranes. Our geochronological and structural results show that the younging direction of accretion was northwards and the subduction zone dipped southwards under the northern margin of the Shuangyingshan micro-continent. This long-lived and continuous accretion process formed the Hanshan accretionary prism. Our field investigations show that the emplacement of the Xiaohuangshan ophiolite was controlled by oceanic crust subduction beneath the forearc accretionary prism of the Shuangyingshan-Mazongshan composite arc to the south. Moreover, we address the age and terrane affiliation of lithologies in the eastern Beishan orogen through detrital zircon geochronology of meta-sedimentary rocks. We provide new information on the ages, subduction polarities, and affiliation of constituent structural units, as well as a new model of tectonic evolution of the eastern Beishan orogen. The accretionary processes and crustal growth of Central Asia were the result of multiple sequences of accretion and collision of manifold terranes.

Key words: Beishan orogenic belt, Xiaohuangshan ophiolite, detrital zircon age, Ar-Ar dating, Altaids

ACCEPTED MANUSCRIPT

1. Introduction

The Altaids lies between the North China and Tarim Cratons in the south, and the Siberian and Eastern European Cratons in the north, and extends from the Urals in the west to the Sikhote-Alin Range in the Russian Far East (Kovalenko et al., 2004; De Jong et al., 2006; Kröner et al., 2007; Safonova et al., 2011; Wilhem et al., 2012; Zhou and Wilde, 2013; Donskaya et al., 2013; Safonova and Santosh, 2014; Kroner et al., 2014) (Fig. 1a); this is the largest accretionary orogenic belt, but it is limited to the period c. 650-250 Ma and does not include the older belts of northernmost Siberia (Şengör et al., 1993; Şengör and Natalin, 1996; Yakubchuk, 2004; Xiao et al., 2009b). The alternative, more appropriate term ‘Central Asian Orogenic Belt (CAOB)’ is now more commonly used, because it covers the period 1.0 Ga to 250 Ma and includes northern Siberia (Mossakovsky et al., 1994; Badarch et al., 2002; Windley et al., 2007; Kröner et al., 2013; Xiao et al., 2013). The continental growth mechanism of the CAOB in Central Asia is now no longer as controversial as it was for the Altaids, when Şengör et al. (1993) suggested that the accretionary growth developed from movement on one subduction zone (or two, Yakubchuk, 2004). But now, there is considerable evidence that the development was mainly achieved by punctuated accretion and collision on multitudes of subduction zones (Mossakovsky et al., 1994; Xiao et al., 2004, 2009a, b; 2010; Windley et al., 2007; He et al., 2014; Safonova and Santosh, 2014; Kröner et al., 2014).

The Beishan orogen, located in the southern CAOB or Altaids, played an important role in the crustal evolution, particularly because it links the Southern Tianshan suture

to the west with the poorly exposed Inner Mongolia Solonker suture to the east (Fig. 1a) (Şengör et al., 1993; Xiao et al., 2003, 2014; Windley et al., 2007; Xu et al., 2009; Jian et al., 2010; Xiao and Santosh, 2014; Guy et al., 2014). Accordingly, the strategically positioned and well-exposed Beishan orogen provides critical information on the final stages of evolution of the orogen just before formation of the terminal suture.

During the last decades numerous studies have focused on the Paleozoic architecture and development of the Beishan (Zuo et al., 1990a, b; 1991, 2003; Liu and Wang, 1995; Ao et al., 2010; Xiao et al., 2010; Song et al., 2012; 2013a, b; Cleven et al., 2015; Tian et al., 2013a, b; Wan et al., 2013; Zheng et al., 2013). Most researchers consider that the Beishan orogen was welded by amalgamation of different terranes that were separated by narrow oceans, broadly similar to present-day SE Asia (Wakita et al., 2013). However, many parts of the orogen have still to be studied in detail, and so many key questions remain to be resolved, such as the subduction polarity of arcs, the emplacement time of ophiolites, the mechanism of exhumation of high-pressure rocks, the structure of accretionary prisms, and the time of ocean closure and terminal collision (Xiao et al., 2004, 2009a; Li, 2006; Jian et al., 2008, 2010; Johnson et al., 2008; Ao et al., 2012; Long et al., 2012a, b; Mao et al., 2012a). Furthermore, it is unclear whether some terranes can be mutually correlated, and whether certain displaced terranes were originally contiguous.

In this paper, we address the subduction polarity of the Xiaohuangshan ocean through detailed field investigations and new zircon and $^{40}\text{Ar}/^{39}\text{Ar}$ geochronological data of meta-sedimentary and meta-igneous rocks. Moreover, we address the age and

terrane affiliation of lithologies in the eastern Beishan orogen through detrital zircon geochronology of meta-sedimentary rocks. With this information we aim to document the structure, make-up and age of several poorly known tectonic belts in eastern Beishan, and integration with published data will enable us to present a new model of tectonic evolution of the Beishan orogen.

2. Regional geology

The Beishan orogen (Fig. 1a) is composed of several EW-trending arc belts that are separated by ophiolite-strewn mélange zones (Zuo et al., 1990a, 1991, 2003; Liu and Wang, 1995) that were displaced by the NE-trending strike-slip Altyn Tagh fault (Wang et al., 2010). In summarizing the regional geology of the Beishan orogen Xiao et al. (2010) showed that it comprises from south to north the following units: the Shibanshan, Shuangyingshan, Mazongshan, Hanshan and Quershan, which are separated respectively by the following (ophiolitic) mélanges: the Liuyuan, Hongliuhe-Xichangjing, Xingxingxia-Xiaohuangshan, and Hongshishan (Fig. 1b). Here we deal only with the geology in the Xiaohuangshan-Yueyashan area (Fig. 2) in which three tectonic units from south to north: the Shuangyingshan, Mazongshan and Hanshan are separated by two ophiolite melanges.

The Shuangyingshan Unit consists of Precambrian to Ordovician shelf carbonates and clastic sediments including limestone, flysch, chert and meta-sandstone; Ao et al. (2012) interpreted this Unit as a micro-continental block. Several granitic intrusions and volcanic rocks crop out in the north of this Unit (Fig. 2). The southern part of this

Unit contains many intrusions situated in Ordovician-Permian calc-alkaline basalts, andesites, rhyolites that are interbedded with clastic sediments and carbonates (Zuo et al., 1990a; Liu and Wang, 1995). Xiao et al. (2010) and Mao et al. (2012b) interpreted this Unit as a multiple long-lived arc that evolved from the Ordovician to the Permian.

The Mazongshan terrane, located between the Xiaohuangshan ophiolite-bearing mélangé to the north and the Yueyashan ophiolite belt to the south (Fig. 2), is composed of Middle/Late Ordovician to Silurian mafic volcanic rocks intercalated with limestones and siliceous slates intercalated with a few mafic-felsic volcanic rocks. These rocks belong to the Baiyunshan Formation on a geological map by the Gansu Bureau of Geology (Anonymous, 1979), interpreted by Ao et al. (2012) as part of an island arc.

The Hanshan terrane is composed of granitic gneisses, felsic volcanic rocks, carbonate sediments and terrestrial clastic rocks that are intercalated with cherts, limestones and volcanic rocks. The metamorphic age of these rocks is poorly known and remains controversial. Based on the fact that whole-rock Rb-Sr and/or Sm-Nd model dates (Zuo et al., 1990a; He et al., 2005) yielded Precambrian ages, some of the rocks were interpreted as a Neoarchean-Paleoproterozoic “Beishan complex”, which rifted from the Tarim-Dunhuang block (Zuo et al., 1990a; Xu et al., 2009). However, the rocks have also been termed the Baishan Formation according to regional stratigraphic correlations and considered to belong to a Paleozoic arc and its accretionary rocks (Anonymous, 1979; Liu and Wang, 1995). Song et al. (2012, 2013b) considered that parts of the Beishan complex belong to a Paleozoic arc, and not a

Precambrian basement. The Hanshan terrane was interpreted by Xiao et al. (2010) as an Early Paleozoic ‘Japan-type complicated arc’.

The Yueyashan ophiolite (Fig. 2) crops out between the Mazongshan and Shuangyingshan Units (Fig. 1) and is composed of an incoherent ophiolitic *mélange* and coherent sedimentary rocks. A weighted mean $^{206}\text{Pb}/^{238}\text{U}$ age of 534.4 ± 3.4 Ma from a plagiogranite in the Yueyashan ophiolite indicates that the ophiolitic ocean floor formed in the early Cambrian. Geochemical data show the Yueyashan ophiolite probably formed in a suprasubduction-zone setting. For detailed information about the Yueyashan ophiolite, see Ao et al. (2012). The Xiaohuangshan ophiolite *mélange* (Figs. 2 and 3) is located between the Mazongshan and Hanshan Units (Fig. 1); the constituent lithological associations and field relationships are described in the next section.

3. Field investigations

The EW-trending Xiaohuangshan ophiolite *mélange* (about 22 km long and 6 km wide) is situated in the Xiaohuangshan fault (TXF) (Fig. 3). A matrix of various schists contains about fifty exotic lenticular blocks that are mainly harzburgites and dunites, and a few olivine pyroxenites, pyroxenites, andesites, and rhyolites. All the ultramafic rocks are intensively serpentized and carbonatized, and some contain chromitites (Anonymous, 1979). The matrix is mainly composed of meta-sandstone, plagioclase-amphibole schist, and chlorite-hornblende schist intercalated with chert and limestone, and quartz-mica schist intercalated with marble. This ophiolite-bearing *mélange* also contains many, multi-stage granites and a few gabbro plutons.

There are three major faults in this area (from north to south, Fig. 3): the Xiaohuangshan North Fault (TXNF), the Xiaohuangshan Fault (TXF), and the Xiaohuangshan South Fault (TXSF). The TXF fault extends for more than 30 km in a NW direction in the west and bends to an E-W direction farther east. This fault is expressed topographically as a straight valley with fault facets. It dips SSW at 45° - 60° , shows top-to-north thrust movement accompanied by sinistral strike-slip, is marked by mylonite and breccia zones, and was intruded by late granitic plutons. The straight-valley TXNF dips SW at 65° - 85° , is a top-to-north thrust that was intruded by dioritic porphyry dikes (Anonymous, 1979). The TXSF fault has different lithologies on either side; from slickensides in serpentinites it is inferred to be a top-to-south thrust (Anonymous, 1977).

The TXNF fault subdivides the ophiolite-bearing mélangé belt into northern and southern parts. Fig. 4 is a cross-section based on our structural studies in the field and in exploratory trenches, combined with drill-core data (Anonymous, 1977). Most ultramafic blocks crop out in the southern part of the mélangé; the long axes of the lenses are almost parallel to the fault strike. The southern part is an EW-trending imbricated thrust sheet, which consists of meta-sandstone, limestone, chert, schist, andesite, rhyolite and ultramafic rocks (Fig. 4). Almost all contacts between the different lithologies are thrusts. Foliations generally dip south at 48° - 75° and are most pervasive in plagioclase-amphibole schist, chlorite-hornblende schist and mica-quartz schist. All the imbricate thrust sheets and the strong foliations indicate north-to-south directed compression.

The entire northern part of the mélangé is characterized by regional-scale tight to isoclinal folds and associated penetrative axial plane cleavage. These folds are asymmetric, verge to the N or NE, their axial surfaces dip S or SW, and their wavelengths locally attain 1-2 km (Fig. 4). Fold axes and associated bedding- cleavage intersection lineations trend NW-SE to W-E, and plunge variably to the NW or E (Fig. 3). The folds are best preserved in the eastern part of the study area; in the western part only fold relics are preserved between the many granitic intrusions. The fold vergence and fabrics indicate that the northern and southern parts of the mélangé underwent north-to-south directed compression.

4. Geochronology

4.1 Methodology

Analytical procedures for $^{40}\text{Ar}/^{39}\text{Ar}$ (step heating argon method) and zircon (U-Pb laser ablation-multicollector, inductively-coupled, plasma-mass spectrometry LA-ICP-MS) analyses are presented in the following sections. Complete data tables are listed in the Appendix. Preferred U-Pb ages are based on $^{238}\text{U}/^{206}\text{Pb}$ ages for zircons younger than 1000 Ma, and $^{207}\text{Pb}/^{206}\text{Pb}$ ages for zircons older than 1000 Ma. For interpretations we considered only ages that have a concordance in the 95%-105% interval ($^{207}\text{Pb}/^{206}\text{Pb}$ age vs. $^{206}\text{Pb}/^{238}\text{U}$ age). The results of the U-Pb zircon ages and the $^{40}\text{Ar}/^{39}\text{Ar}$ analyses are plotted in Figures 5 and 6, and all data are listed in Tables A and B in the Appendix.

4.1.1 Analytical Procedures: $^{40}\text{Ar}/^{39}\text{Ar}$ dating

Five whole-rock samples were crushed and sieved between 250 and 400 μm fractions and then thoroughly washed with distilled water and acetone. Muscovite, hornblende and biotite were carefully handpicked using a binocular microscope to reduce any visible impurities after paramagnetic separation, and these minerals were cleaned in 5% HF for 10 minutes to reduce melt inclusions and adhering glass. Samples were wrapped in aluminum foil and irradiated together with Bern4M Muscovite standards monitored for 24 hours in position B4 of the 49-2 reactor, Beijing, China. The reference age for the Bern4M is 18.69 ± 0.36 Ma (Baksi et al., 1996; McDougal and Harrison, 1999).

Total fusion of standards and high-resolution incremental heating analyses of samples were performed on a MM5400 mass spectrometer operating in a static mode at the $^{40}\text{Ar}/^{39}\text{Ar}$ Geochronology Laboratory, Institute of Geology and Geophysics, Chinese Academy of Sciences, Beijing. In order to reveal and mitigate the effects of alteration and/or partial Ar loss, high resolution incremental heating (more than 17 steps for each sample) was the preferred mode of analysis because of the internal reliability criteria offered by the age spectrum technique (McDougal and Harrison, 1999). Samples were degassed at 650 $^{\circ}\text{C}$ for 30 minutes before being incrementally heated in a double vacuum furnace to reduce air contamination. The gases released during each step were purified by 2 SAES NP10 getters (operated at 350 $^{\circ}\text{C}$ and 100 $^{\circ}\text{C}$, respectively) before introduction into the mass spectrometer for Ar isotope determinations. The ^{40}Ar , ^{39}Ar , ^{38}Ar , ^{37}Ar , and ^{36}Ar isotopic abundances were determined through linear extrapolation at time zero of peak intensities. The data were

corrected for system blanks, mass discriminations, interfering Ca, K-derived argon isotopes, and the decay of ^{37}Ar after the time of irradiation. The decay constant used throughout the calculations was $\lambda = (5.543 \pm 0.010) \times 10^{-10} \text{ a}^{-1}$, as recommended by Steiger and Jäger (1977). Details of the analysis and data processing procedures are given in Wang et al. (2006) and Yang et al. (2008). Plateau ages were defined as three or more contiguous steps corresponding to a minimum of 50% of the ^{39}Ar released that showed no statistically difference in 95% confidence level (McDougall and Harrison, 1999).

4.1.2 Analytical Procedures: zircon U-Pb LA -ICP-MS dating

Zircon crystals were obtained from crushed rocks with a combination of heavy liquid and magnetic separation techniques. Individual crystals were handpicked and mounted in epoxy resin. Experiments were carried out at the MC-ICP-MS laboratory of the Tianjin Institute of Geology and Mineral Resources using an UP193-FX laser-ablation system equipped with a 193 nm ArF-excimer laser in connection with a Thermo Fisher ICPMS. Helium was used as the carrier gas to enhance the transport efficiency of the ablated material. The analyses were conducted with a beam diameter of 50 μm and a typical ablation time of about 30s for 200 cycles for each measurement, as well as a 10 Hz repetition rate and a laser power of 100mJ/pulse (Wu et al., 2006). Uranium, Th and Pb concentrations were calibrated by using ^{29}Si as an internal standard and NIST SRM 610 as an external standard. $^{207}\text{Pb}/^{206}\text{Pb}$ and $^{206}\text{Pb}/^{238}\text{U}$ ratios were calculated using GLITTER 4.0 (Jackson et al., 2004), which was then corrected with Harvard zircon 91500 as an external standard. The $^{207}\text{Pb}/^{235}\text{U}$ ratios were calculated from the values of

$^{207}\text{Pb}/^{206}\text{Pb}$ and $^{206}\text{Pb}/^{238}\text{U}$. Common Pb was corrected according to the method of Andersen (2002). The weighted mean U-Pb ages and Concordia plots were processed using ISOPLOT 3.0. More detailed procedures can be found in Xie et al. (2008).

4.2 Results

Complete $^{40}\text{Ar}/^{39}\text{Ar}$ incremental heating data and LA-ICP-MS zircon U-Pb data are in Appendix Table A and B, respectively. The sample names, locations and petrology/mineral assemblages are described in Appendix C.

4.2.1 $^{40}\text{Ar}/^{39}\text{Ar}$ dating

Complete $^{40}\text{Ar}/^{39}\text{Ar}$ incremental heating data are in Appendix Table A, and age spectra and isotope correlation (inverse isochron) diagrams are illustrated in Figure 6. For each sample the argon release age spectra and inverse isochrones are presented, and both of their uncertainties are given at a 2σ level.

Samples 09AB09 and 09AB11 are mica schist and granitic gneiss, respectively. Two muscovite samples picked out from 09AB09 and 09AB11 yield concordant age spectra (Fig. 6). Nine consecutive steps, which account for 81% of the total ^{39}Ar released from 09AB09, define a plateau age of 455 ± 3 Ma (MSWD = 2.07) (Fig. 6A). An inverse isochron age of 458 ± 5 Ma (MSWD = 1.78) (Fig. 6a), calculated from these plateau steps, is in agreement with the plateau age. The $^{40}\text{Ar}/^{36}\text{Ar}$ intercept of 181.64 ± 99.94 is apparently lower than the atmospheric value (295.5), implying that the background contribution in the data should be considered when interpreting the plateau ages. The data yield a fine $^{40}\text{Ar}/^{39}\text{Ar}$ age spectrum, suggesting a closed system behavior. We

regard the inverse isochron age as being more objective because no assumptions are made about the initial $^{40}\text{Ar}/^{36}\text{Ar}$ ratio. Thus 458 ± 5 Ma represents the cooling age of muscovite 09AB09. Nine consecutive steps, which account for 88.9% of the total ^{39}Ar released from 09AB11, define a plateau age of 431 ± 3 Ma (MSWD = 1.31) (Fig. 6B). An inverse isochron age of 432 ± 3 Ma (MSWD = 1.48) (Fig. 6b), calculated from all steps that formed the plateau, is indistinguishable from the plateau age. The $^{40}\text{Ar}/^{36}\text{Ar}$ intercept of 290.34 ± 34.16 is in agreement with the air $^{40}\text{Ar}/^{36}\text{Ar}$ ratio, indicating that there is no resolvable excess argon contamination. Therefore, the inverse isochron age is more objective, because no assumptions are made about the initial $^{40}\text{Ar}/^{36}\text{Ar}$ ratio. This result represents an age of 432 ± 3 Ma for the muscovite crystallization.

Both samples 10ASJ03 and 10ASJ10 are granitic diorites. Two hornblende samples picked out from 10ASJ03 and 10ASJ10 yield well-defined age spectra, about 99% of ^{39}Ar released giving plateau ages of 425 ± 3 Ma (MSWD = 1.64) and 429 ± 3 Ma (MSWD = 0.95) respectively (Fig. 6C, E). The inverse isochron ages of 426 ± 3 Ma for 10ASJ03 and 430 ± 3 Ma for 10ASJ10 are indistinguishable from their respective plateau ages. The initial values of $^{40}\text{Ar}/^{36}\text{Ar}$ of these samples are consistent with the atmospheric $^{40}\text{Ar}/^{36}\text{Ar}$ ratio (295.5) (Fig. 6c, e). Considering the analytical errors, these two $^{40}\text{Ar}/^{39}\text{Ar}$ ages from samples 10ASJ03 and 10ASJ10 are almost identical. The results suggest a minimum age of about 426 ± 3 Ma for the hornblende crystallization and granitic gneiss formation.

Biotite picked from granitic gneiss sample (10ASJ08) yields concordant age spectra accounting for 72 % of released ^{39}Ar (Fig. 6D). The data show a plateau age of 367 ± 2

Ma (MSWD = 0.57) (Fig. 6D) and an inverse isochron age of 368 ± 3 Ma ($n = 7$, MSWD = 0.48) (Fig. 6d). The initial $^{40}\text{Ar}/^{36}\text{Ar}$ value of 290.99 ± 8.86 is consistent with the atmospheric value of 295.5. We regard the inverse isochron age as being more objective, because no assumptions are made about the initial $^{40}\text{Ar}/^{36}\text{Ar}$ ratio. Thus, 368 ± 3 Ma represents the cooling age of biotite from sample 10ASJ08.

4.2.2 Zircon U-Pb LA-ICP-MS dating

Representative rocks from the Baishan, Baiyunshan, and Baihu Formations were sampled for separation of zircon for U-Pb analyses (Fig. 2).

Granitic Gneisses

Three samples (10ASJ08, granitic gneiss; 10ASJ10, gneissic diorite; 09AB11, granitic gneiss) were collected from the Lower Baishan Formation and the contact with the Baiyunshan Formation for analyses (Figure 2). Zircons from all samples are semi-transparent, 50-150 μm in length, and have aspect ratios of $\sim 1:1$ to $2:1.1$. In cathodoluminescence (CD) images most zircons are characterized by magmatic concentric zones. Fourteen zircon spot analyses were analyzed from sample 10ASJ08. All the measured Pb/U ratios are concordant within analytical errors, yielding a concordia age of 418 ± 5 Ma (1σ , MSWD = 4.0) (Fig. 5), which is interpreted as the time of crystallization of the granitic pluton (sample 10ASJ08). Twenty zircon spot analyses were analyzed from sample 10ASJ10. All the measured Pb/U ratios are concordant within analytical errors, yielding a concordia age of 424 ± 3 Ma (1σ , MSWD = 1.9) (Fig. 5), which is interpreted as the time of crystallization of the granitic

pluton (sample 10ASJ10). Nineteen spot analyses were made of nineteen zircons from sample 09AB11, sixteen of which yield a concordia age of 713 ± 6 Ma (1σ , MSWD = 2.9) (Fig. 5), which we interpret as the main time of crystallization of the granitic gneiss. One spot analysis shows a concordia age of 1132 ± 7 Ma, which we interpret as an inherited age. Two zircon spot analyses show a weight mean age of 515 ± 7 Ma, which possibly indicates the time of dike intrusion.

Meta-sedimentary rocks

Four sedimentary samples were collected from the Lower Baishan Formation and Baiyunshan Formation for detrital zircon analyses (Fig. 2).

Sample 09AB10 is a greenschist-facies, quartz-rich schist from the Baiyunshan Formation (Fig. 2). 85 individual zircon grains were analyzed, of which 85 were <5% discordant. The age distribution shows prominent Phanerozoic peaks at 462 Ma and 429 Ma, with three small Proterozoic peaks at 647 Ma, 718 Ma and 794 Ma (Fig. 7). The sample yields an Early Silurian maximum depositional age of 432 ± 5 Ma defined by a cluster of 13 ages that overlap within uncertainty. Sample 10ASJ14 is a low-grade meta-sandstone from the Baiyunshan Formation (Fig. 2). 60 individual zircon grains were analyzed, of which 57 were <5% discordant. The age distribution shows prominent Proterozoic peaks at 919 Ma and 2430 Ma, with a small peak at 1520 Ma (Fig. 7). One concordant age yields a date of 509 ± 5 Ma, which indicates that the maximum time of deposition was in the Middle Cambrian. Sample 10ASJ24 is a sandstone from the Shuangyingshan Formation (Fig. 2), which provided 49 individual zircon grains for analysis, of which 47 were < 5% discordant. The age distribution

shows prominent Proterozoic peaks at 927 Ma and 2475 Ma, with small peaks at 575 Ma and 3142 Ma (Fig. 7). One concordant age yields a date of 516 ± 5 Ma, which indicates the maximum time of deposition was in the Middle Cambrian. Sample 10ASJ27 is low-grade meta-siltstone from the Baihu Group (Fig. 2); 100 individual zircon grains were analyzed, of which 73 were <5% discordant. The age distribution shows prominent Proterozoic peaks at 1828 Ma and 1673 Ma (Fig. 7) and a maximum depositional age of 1329 ± 18 Ma defined by a cluster of five peaks that overlap within uncertainty.

5. Discussion

5.1 The affinity of the Shuangyingshan terrane

The tectonic evolution of the Beishan orogen has so far been not well understood, largely due to lack of consensus about different ideas about the tectonic affinity of the main terranes. The samples 10ASJ14, 10ASJ24 and 10ASJ27 are components of the Shuangyingshan terrane (Fig. 2). The U-Pb cumulative age probability plots of detrital zircons of the three samples are comparable with those from the western Shuangyingshan (WS), as shown in Fig. 7b; the detrital age distribution shows prominent peaks at 927 Ma, 798 Ma and 2500 Ma with small peaks in the period 490 Ma to 741 Ma (Fig. 7b). The detrital age distributions of sedimentary rocks from northeastern Tarim show prominent peaks at 800 Ma, 1800 Ma, 2000 Ma and 2500 Ma, with no small peaks in the period 490 Ma to 741 Ma (Zhang et al., 2011, 2012) (Fig. 7c). This indicates that Shuangyingshan was a micro-continent distant from the northeastern

Tarim block after about 741 Ma, and thus could not have been a viable sedimentary source. In other words, before 741 Ma detrital zircons in the Shuangyingshan micro-continent and northeastern Tarim had the same sedimentary provenance, because the two blocks were probably co-joined. The detrital zircon age distributions of Neoproterozoic sediments from the Shuangyingshan micro-continent yield a maximum depositional age at 1170-1129 Ma with prominent peaks at about 1800 Ma and small peaks at 2000 Ma and 2500 Ma (Fig. 7b). This detrital zircon age distribution is similar to that of the Alxa block to the east (Zhang et al., 2012) suggesting that the Shuangyingshan micro-continent was probably linked with the Tarim and Alxa blocks before 741 Ma.

Accordingly, we consider that the Shuangyingshan terrane rifted from the Tarim-Alxa block at about 741 Ma and became an independent micro-continent in the Paleo-Asian Ocean after that time.

5.2 Formation of the Hanshan accretionary prism

The Hanshan terrane is composed of granitic gneiss, felsic volcanic rocks, carbonates and terrestrial clastic rocks that are intercalated with cherts, limestones and volcanic rocks. Because whole-rock Rb-Sr ages and/or Sm-Nd model ages (Zuo et al., 1990a; He et al., 2005) were Precambrian, some of the rocks were interpreted as a Neoproterozoic-Paleoproterozoic “Beishan complex”, rifted from the Tarim-Dunhuang block (Zuo et al., 1990a; Xu et al., 2009). These rocks were grouped under the term ‘Baishan Formation’ by regional stratigraphic correlations and from available geochemical and isotopic data were considered to belong to a Paleozoic arc and its

associated accreted rocks (Anonymous, 1979; Liu and Wang, 1995; Xiao et al., 2010).

In order to constrain the affinity of the Hanshan terrane and its relationship with the Hanshan terrane and Xiaohuangshan ophiolite, we collected six samples from south to north across the Xiaohuangshan ophiolitic belt for zircon U/Pb and Ar/Ar dating; 09AB09, 09AB10, 09AB11, 10ASJ10, 10ASJ03 and 10ASJ08 (Fig. 2), and the implications of their isotopic ages are discussed below.

The Ar-Ar date on muscovite from 09AB09 defines an inverse isochron age of 458 ± 5 Ma. Thin-sections show that the muscovite was oriented during the deformation (Fig. 8b), suggesting it is a regional metamorphic mineral associated with the deformation. Therefore, this age is interpreted as the cooling formation age of the muscovite, which is close to the peak temperatures of the blueschist facies metamorphism of the mica schist (320-450°C). However, this sample has an Ar loss problem, and the real metamorphism age should be before 458 Ma.

Sample 09AB10 is a mica-quartz schist that forms the matrix of the Xiaohuangshan ophiolitic mélangé. Analyses of detrital zircons from 09AB10 yield an Early Silurian maximum depositional age of 432 ± 5 Ma, which points to a main Phanerozoic peak at 462 Ma and three small Proterozoic peaks at 647 Ma, 718 Ma and 794 Ma (Figs. 5 and 7a). These peaks are totally different from those of samples from the Shuangyingshan micro-continent that have prominent peaks at 927 Ma (Fig. 7b). This is explicable if the Mazongshan arc was located between the Shuangyingshan micro-continent and the Xiaohuangshan mélangé, and thus the sedimentary source was probably from the Mazongshan arc (Figs. 9a, and b).

The banded gneiss sample 09AB11 yields a zircon U-Pb concordia age of 713 ± 6 Ma ($n = 16$) and a young weighted mean age of 515 ± 7 Ma ($n = 2$). Ar-Ar dating of muscovite from the same sample 09AB11 yields an inverse isochron age of 432 ± 3 Ma (MSWD = 1.48) (Fig. 6b), which is interpreted as a muscovite cooling age that was affected by intrusions in the Hanshan terrane.

The gneissic diorite samples (10ASJ10 and 10ASJ03) are components of the Hanshan terrane. The U-Pb zircon dates from sample 10ASJ10 yield a concordia age of 424 ± 3 Ma (Fig. 5c) and the Ar-Ar date of hornblende from 10ASJ10 defines an inverse isochron age of 430 ± 3 Ma (Fig. 6e), and an Ar-Ar hornblende date from 10ASJ03 gives an inverse isochron age of 426 ± 3 Ma (Fig. 6c). The Ar-Ar ages are consistent with the U-Pb zircon ages within the error range; the former are interpreted as the time of formation of the diorite intrusions. In thin sections the hornblendes define a weak foliation suggesting they are syn-tectonic (Fig. 8a).

Sample 10ASJ08 is a gneissic granite from which zircons yield a U-Pb concordia age of 418 ± 5 Ma (1σ , MSWD = 4.0) (Fig. 5), which we interpret as the time of crystallization of the granitic pluton. The Ar-Ar date of biotite from sample 10ASJ08 defines an inverse isochron age of 368 ± 3 Ma (Fig. 6d), which we interpret as the metamorphic crystallization age of the biotite. In thin sections aligned biotites mark a weak foliation, thus it is likely this is a syn-tectonic metamorphic phase (Fig. 8c). The closure temperature of biotite is low (300-350 °C), and thus is able to record a low-grade metamorphic event caused by accretion.

A summary plot of all the geochronological data across the Mazongshan arc axis

with its extensive andesite outcrops clearly shows that the ages become younger from south to north (Figs. 2 and 9c). A combination of all the geology, petrology and geochronology of the Hanshan terrane (Anonymous, 1979; Zuo et al., 1991; Liu and Wang, 1995; Xiao et al., 2010) indicates that it is an accretionary prism, which formed from the Silurian to the Devonian (457-367 Ma) on the northern margin of the Shuangyingshan-Mazhongshan composite arc (Fig. 9c).

5.3 Formation of the Xiaoshaoshan ophiolite

The original setting, formation age, and the time and mechanism of emplacement are keys to understand the origin of ophiolites. The Xiaohuangshan ophiolite either formed in a mid-ocean-ridge of the Paleo-Ocean between the Tarim craton to the south and the Kazakhstan craton to the north (Zuo et al., 1990b), or in a suprasubduction zone below an arc similar to many in the current Southwest Pacific Ocean (Xiao et al., 2010; Wakita et al., 2013). The Xiaohuangshan ophiolite is a typical *mélange* characterized by a block-in-matrix structure (Fig. 3). The blocks are mainly harzburgites, andesites, rhyolites and limestones, the geochemistry of which indicates an arc setting (Zheng et al., 2013). The formation age of this ophiolite ranges from 485 ± 75 Ma (Sm-Nd isochron age of gabbro) (Song et al., 2008) to 334.6 ± 4 Ma on basalt, and 345 ± 14 Ma on gabbro (SHRIMP U-Pb age) (Zheng et al., 2013). The Xiaohuangshan Ocean probably formed in the Carboniferous (Zheng et al., 2013). However, our zircon U-Pb and Ar/Ar ages of deformed granitic gneiss and metasedimentary rocks located on both sides of the Xiaohuangshan ophiolitic belt are not younger than Early Carboniferous. So we prefer to interpret the Xiaohuangshan Ocean as a small, short-lived oceanic basin

formed on the Hanshan accretionary prism, possibly caused by slab rollback in the north (Fig. 9d). As a result of our investigations we consider in principle that a thin ophiolite is a relict fragment of oceanic crust scraped off during subduction erosion in a trench before it was thrust into an accretionary prism (Kimura and Ludden, 1995; Stern, 2011). Locally, it was closure of the Xiaohuangshan Ocean that was responsible for the emplacement of the Xiaohuangshan ophiolite into the Hanshan accretionary prism in the Late Carboniferous (Fig. 9e).

5.4 Tectonic evolution of the Beishan orogen

The Beishan orogenic collage is a typical accretionary orogen composed of magmatic arcs and ophiolitic mélanges; the accretionary orogenesis lasted perhaps from the Late Cambrian to the Late Permian (Xiao et al., 2010; Ao et al., 2012; Guo et al., 2012; Mao et al., 2012; Tian et al., 2013b). An appropriate evolutionary tectonic model of the Beishan orogen by Xiao et al. (2010) is updated here to include the latest data, which better constrain the nature and timing of the main terranes in the eastern Beishan. Consequently, we are able to construct a new model for the tectonic evolution of the eastern Beishan (Fig. 9), in which the main orogenic process was accretion of an arc/accretionary prism to a composite arc. Our model of tectonic evolution, illustrated in Fig. 9, is as follows:

In the Cambrian-Ordovician subduction of the Yueyashan ocean created the Mazongshan volcanic arc and accretionary complex to the north of the Shuangyingshan micro-continent. In the Late Ordovician-Early Silurian (Fig. 9b), the Yueyashan Ocean closed, causing the Yueyashan ophiolite to be emplaced onto the Mazongshan arc (Ao

et al., 2012). Then the Shuangyingshan micro-continent and Mazhongshan arc were welded together into a composite arc. The Paleo-Asian Ocean began to subduct to the south beneath the composite arc at this time (Fig. 9c). In the Late Silurian-Devonian, all the geochronological data indicate that the accretion become younger towards the north away from the northern margin of the Shuangyingshan micro-continent; this continuous accretionary process created the Hanshan accretionary prism. In the Early Carboniferous (Fig. 9d) extension took place within the Hanshan accretionary prism forming a small Xiaohuangshan intra-arc oceanic basin in which basalts and gabbros were emplaced at 336 Ma and 345 Ma, respectively (Zheng et al., 2013). We suspect that this extension was caused by rollback of the subducted oceanic plate to the north. In the Late Carboniferous (Fig. 9e) closure of the Xiaohuangshan oceanic basin caused the Xiaohuangshan ophiolite to be thrust into the Hanshan accretionary prism.

In conclusion, we propose that the accretionary processes and continental growth in the southern (present coordinates) Central Asian Orogenic Belt were characterized by semi-continuous episodes of subduction-accretion with different subduction polarities. The currently available evidence negates the inappropriate old idea of just long-lasting evolution of one subduction zone (Şengör et al., 1993). Some small oceans probably existed within the overall Paleo-Asian Ocean, but nevertheless the major process of crustal growth was long-lived, uni-directional forearc accretion that gave rise to many arcs and their associated accretionary prisms. We conclude that the main accretionary mechanism and continental growth in Central Asia was multiple stages of consecutive accretion and collision.

6. Conclusions

Our field work combined with new detrital zircon analyses, Ar-Ar dating and structural studies in eastern Beishan, integrated with results from previous investigations, demonstrate the following relationships:

(1) Before the Neoproterozoic the Shuangyingshan terrane was a micro-continent, which shared distinctive age peaks with, and was a contiguous part of, the northeastern Tarim block, but at ~741 Ma it rifted from the Tarim block, and thus became an independent different provenance for detrital sediment.

(2) The Hanshan terrane is an accretionary prism, which accreted continuously from the Silurian to the Devonian (457-367 Ma) on the northern margin of the Shuangyingshan-Mazhongshan composite arc. The younging direction of accretion was from south to north, and it continued to grow until the Late Carboniferous.

(3) The Xiaohuangshan Ocean started as an intra-arc basin within a forearc accretionary prism in the Early Carboniferous, probably caused by slab rollback. The Xiaohuangshan Ocean probably closed in the Late Carboniferous when the Xiaohuangshan ophiolite was emplaced into the Hanshan accretionary prism. The accretion-emplacement process may have been caused by oceanic subduction below the accretionary prism to the south.

(4) The processes of accretionary continental growth in Central Asia were dominated by semi-continuous, multiple episodes of accretion and collision. We are confident that this conclusion is viable, because in the last two decades it has been tested by a huge body of fieldwork (which is necessary if speculative models are to be tested) by

international researchers from far and wide, which has led to considerable quantitative laboratory data, which have evaluated and tested competing models, concluding that accretion can only have taken place by multiple and successive episodes of subduction.

ACCEPTED MANUSCRIPT

Acknowledgements

We thank guest editor Yunpeng Dong and two anonymous referees for their comments and corrections, which greatly improved the manuscript. This research was supported by grants from the Natural Science Foundation of China (grants 41390441, 41230207, 41202150 and 41190075). Contribution to IGCP 592.

Captions

Fig. 1. (a) Map showing the location of the Beishan area in the south of the Central Asian Orogenic Belt. (b) Schematic geological map of the Beishan collage showing the main, named tectonic Units (modified after (Zuo et al., 1990b; Xu et al., 2009; Xiao et al., 2010)). Box shows the location of Figure 2.

Fig. 2. Geological map of the Xiaohuangshan-Yueyashan area, which marks the positions of dated samples, the Xiaohuangshan ophiolite, and location of Figure 3. All the geochronological data from this study demonstrate that the accretionary belts young progressively from south to north.

Fig. 3. Geological map of the Xiaohuangshan ophiolite-bearing mélangé (modified after Anonymous (1979)). The boxes show the location of Figure 4.

Fig. 4. Schematic section across the Xiaohuangshan ophiolite mélangé. Bedding/foliation and fold cleavage largely dip to the south consistent with accretion to the north (Fig. 2), and in consequence the subduction zone dipped to the south.

Fig. 5. U-Pb Concordia age diagrams of zircons in samples from Eastern Beishan.

Fig. 6. Age spectra (A-E), and isotope correlation (a-e) diagrams of samples from the

Xiaohuangshan area. The plateau ages are indicated by dark lines. Solid rectangles denote the steps used in fitting the inverse isochrons. 2 sigma errors are quoted for the points plotted in isotope correlation diagrams (a-e).

Fig. 7. U-Pb cumulative age probability plots of detrital zircons. (a) from the Hanshan accretionary prism, (b) from the Shuangyingshan micro-continent, (3) from NE Tarim. MDA = maximum depositional age, WS = Western Beishan. □ data of this study, other data after [1](Song et al., 2013b), [2](Zhang et al., 2012), [3](Zhang et al., 2011)

Fig. 8. Micrographs of gneissic diorite (a, 10ASJ03), mica quartz schist (b, 09AB09) and gneissic granite (c, 10ASJ 08) under cross-polarized light demonstrating a weak preferred orientation of hornblende in (a), preferred orientation of muscovite in (b), and a weak preferred orientation of biotite in (c).

Fig. 9. Schematic model to explain the tectonic evolution of the eastern Beishan orogen in four stages from the Cambro-Ordovician to the Late Carboniferous. * data from this study. For details see the discussion in the text.

References

- Andersen, T., 2002. Correction of common lead in U–Pb analyses that do not report ^{204}Pb . *Chemical Geology* 192, 59-79.
- Anonymous, 1977. The geological survey report of chromite-bearing ultramafic rocks in the north of Yueyashan, Ejina Banner, Gansu province. 1-65 (in Chinese).
- Anonymous, 1979. Geological map of the Lujing Region, China, 1:200,000, The Geomechanics and Regional Geological Team of the Gansu Bureau of Geology (in Chinese).
- Ao, S.J., Xiao, W.J., Han, C.M., Li, X.H., Qu, J.F., Zhang, J.E., Guo, Q.Q., Tian, Z.H., 2012. Cambrian to early Silurian ophiolite and accretionary processes in the Beishan collage, NW China: implications for the architecture of the southern Altai. *Geological Magazine* 149, 606-625.
- Ao, S.J., Xiao, W.J., Han, C.M., Mao, Q.G., Zhang, J.E., 2010. Geochronology and geochemistry of Early Permian mafic-ultramafic complexes in the Beishan area, Xinjiang, NW China: Implications for late Paleozoic tectonic evolution of the southern Altai. *Gondwana Research* 18, 466-478.
- Badarch, G., Cunningham, W.D., Windley, B.F., 2002. A new terrane subdivision for Mongolia: implications for the Phanerozoic crustal growth of Central Asia. *Journal of Asian Earth Sciences* 21, 87-110.
- Baksi, A.K., Archibald, D.A., Farrar, E., 1996. Intercalibration of $^{40}\text{Ar}/^{39}\text{Ar}$ dating standards. *Chemical Geology* 129, 307-324.
- Cleven, N.R., Lin, S.F., Xiao, W.J., 2015. The Hongliuhe fold-and-thrust belt: Evidence of terminal collision and suture-reactivation after the Early Permian in the Beishan orogenic collage, Northwest China. *Gondwana Research*, 27, 796-810.
- De Jong, K., Xiao, W.J., Windley, B.F., Masago, H., Lo, C.H., 2006. Ordovician $^{40}\text{Ar}/^{39}\text{Ar}$ phengite ages from the blueschist-facies Ondor Sum subduction-accretion complex (Inner Mongolia) and implications for the Early

- Paleozoic history of continental blocks in China and adjacent areas. *American Journal of Science* 306, 799-845.
- Donskaya, T.V., Gladkochub, D.P., Mazukabzov, A.M., Ivanov, A.V., 2013. Late Paleozoic-Mesozoic subduction-related magmatism at the southern margin of the Siberian continent and the 150 million-year history of the Mongol-Okhotsk Ocean. *Journal of Asian Earth Sciences* 62, 79-97.
doi:10.1016/j.jseaes.2012.07.023.
- Guo, Q., Xiao, W., Windley, B.F., Mao, Q., Han, C., Qu, J., Ao, S., Li, J., Song, D., Yong, Y., 2012. Provenance and tectonic settings of Permian turbidites from the Beishan Mountains, NW China: Implications for the Late Paleozoic accretionary tectonics of the southern Altaids. *Journal of Asian Earth Sciences* 49, 54-68.
- Guy, A., Schulmann, K., Clauer, N., Hasalova, P., Seltmann, R., Armstrong, R., Lexa, O., Benedicto, A., 2014. Late Paleozoic-Mesozoic tectonic evolution of the Trans-Altai and South Gobi Zones in southern Mongolia based on structural and geochronological data. *Gondwana Research* 25, 309-337.
- He, C., Santosh, M., Chen, X., Li, X., 2014. Crustal growth and tectonic evolution of the Tianshan orogenic belt, NW China: A receiver function analysis. *Journal of Geodynamics* 75, 41-52. doi:10.1016/j.jog.2014.02.004.
- He, S.P., Zhou, H.W., Ren, B.C., Yao, W.G., Fu, L.P., 2005. Crustal evolution of Palaeozoic in Beishan area, Gansu and Inner Mongolia, China. *Northwestern Geology (in Chinese with English abstract)*, 38, 6-15.
- Jackson, S.E., Pearson, N.J., Griffin, W.L., Belousova, E.A., 2004. The application of laser ablation-inductively coupled plasma-mass spectrometry to in situ U–Pb zircon geochronology. *Chemical Geology* 211, 47-69.
- Jian, P., Liu, D., Kröner, A., Windley, B.F., Shi, Y., Zhang, F., Shi, G., Miao, L., Zhang, W., Zhang, Q., Zhang, L., Ren, J., 2008. Time-scale of an early to mid-Paleozoic orogenic cycle of the long-lived Central Asian Orogenic Belt, Inner Mongolia of China: implications for continental growth. *Lithos* 101, 233-259.

- Jian, P., Liu, D., Kröner, A., Windley, B.F., Shi, Y., Zhang, W., Zhang, F., Miao, L., Zhang, L., Tomurhuu, D., 2010. Evolution of a Permian intraoceanic arc–trench system in the Solonker suture zone, Central Asian Orogenic Belt, China and Mongolia. *Lithos* 118, 169-190.
- Johnson, C.L., Amory, J.A., Zinniker, D., Lamb, M.A., Graham, S.A., Affolter, M., Badarch, G., 2008. Sedimentary response to arc-continent collision, Permian, southern Mongolia. *Geological Society of America Special Papers* 436, 363-390.
- Kovalenko, V.I., Yarmolyuk, V.V., Kovach, V.P., Kotov, A.B., Kozakov, I.K., Salnikova, E.B., Larin, A.M., 2004. Isotope provinces, mechanisms of generation and sources of the continental crust in the Central Asian mobile belt: geological and isotopic evidence. *Journal of Asian Earth Sciences* 23(5), 605-627.
doi:[http://dx.doi.org/10.1016/S1367-9120\(03\)00130-5](http://dx.doi.org/10.1016/S1367-9120(03)00130-5).
- Kröner, A., Windley, B.F., Badarch, G., Tomurtogoo, O., Hegner, E., Jahn, B.M., Gruschka, S., Khain, E.V., Demoux, A., Wingate, M.T.D., 2007. Accretionary growth and crust formation in the Central Asian Orogenic Belt and comparison with the Arabian-Nubian shield. *Geological Society of America Memoirs* 200, 181-209. doi:10.1130/2007.1200(11).
- Kröner, A., Alexeiev, D.V., Rojas-Agramonte, Y., Hegner, E., Wong, J., Xia, X., Belousova, E., Mikolaichuk, A.V., Seltmann, R., Liu, D., Kiselev, V.V., 2013. Mesoproterozoic (Grenville-age) terranes in the Kyrgyz North Tianshan: Zircon ages and Nd-Hf isotopic constraints on the origin and evolution of basement blocks in the southern Central Asian Orogen. *Gondwana Research* 23, 272-295.
- Kröner A., Kovach, V., Belousova, E., Hegner, E., Armstrong, R., Dolgoplova, A., Seltmann, R., Alexeiev, D.V., Hoffmann, J.E., Wong, J., Sun, M., Cai, K., Wang, T., Tong, Y., Wilde, S.A., Degtyarev, K.E., Rytsk, E., 2014. Reassessment of continental growth during the accretionary history of the Central Asian Orogenic Belt. *Gondwana Research* 25, 103-125.
- Kimura, G., Ludden, J. 1995. Peeling oceanic crust in subduction zones. *Geology* 23, 217-220.

- Li, J.Y., 2006. Permian geodynamic setting of Northeast China and adjacent regions: closure of the Paleo-Asian Ocean and subduction of the Paleo-Pacific Plate. *Journal of Asian Earth Sciences* 26, 207-224.
- Liu, X.Y., Wang, Q., 1995. Tectonics and evolution of the Beishan orogenic belt, West China. *Geological Research* (in Chinese with English abstract) 10, 151-165.
- Long, X., Yuan, C., Sun, M., Safonova, I., Xiao, W., Wang, Y., 2012a. Geochemistry and U-Pb detrital zircon dating of Paleozoic graywackes in East Junggar, NW China: Insights into subduction-accretion processes in the southern Central Asian Orogenic Belt. *Gondwana Research* 21, 637-653.
- Long, X., Yuan, C., Sun, M., Xiao, W., Wang, Y., Cai, K., Jiang, Y., 2012b. Geochemistry and Nd isotopic composition of the Early Paleozoic flysch sequence in the Chinese Altai, Central Asia: Evidence for a northward-derived mafic source and insight into Nd model ages in accretionary orogen. *Gondwana Research* 22, 554-566.
- Mao, Q., Xiao, W., Fang, T., Wang, J., Han, C., Sun, M., Yuan, C., 2012a. Late Ordovician to early Devonian adakites and Nb-enriched basalts in the Liuyuan area, Beishan, NW China: Implications for early Paleozoic slab-melting and crustal growth in the southern Altaids. *Gondwana Research* 22, 534-553.
- Mao, Q., Xiao, W., Windley, B.F., Han, C., Qu, J., Ao, S., Zhang, J.E., Guo, Q., 2012b. The Liuyuan complex in the Beishan, NW China: a Carboniferous–Permian ophiolitic fore-arc sliver in the southern Altaids. *Geological Magazine* 149, 483-506.
- McDougal, I., Harrison, T.M., 1999. *Geochronology and Thermochronology by the $^{40}\text{Ar}/^{39}\text{Ar}$ Method*, 2nd ed. Oxford University Press. USA.
- Mossakovsky, A.A., Ruzhentsov, S.V., Samygin, S.G., Kheraskova, T.N., 1994. The central Asian fold belt: geodynamic evolution and formation history. *Geotectonics* 27, 455-473.
- Safonova, I., Seltmann, R., Kroener, A., Gladkochub, D., Schulmann, K., Xiao, W., Kim, J., Komiya, T., Sun, M., 2011. A new concept of continental construction in the Central Asian Orogenic Belt (compared to actualistic examples from the

- Western Pacific). *Episodes* 34(3), 186-196.
- Safonova, I.Y., Santosh, M., 2014. Accretionary complexes in the Asia-Pacific region: Tracing archives of ocean plate stratigraphy and tracking mantle plumes. *Gondwana Research* 25, 126-158.
- Şengör, A.M.C., Natalin, B.A., 1996. Turkic-type orogeny and its role in the making of the continental crust. *Annual Review of Earth and Planetary Sciences* 24, 263-337.
- Şengör, A.M.C., Natalin, B.A., Burtman, V.S., 1993. Evolution of the Altiid Tectonic Collage and Paleozoic Crustal Growth in Eurasia. *Nature* 364, 299-307.
- Song, D., Xiao, W., Han, C., Li, J., Qu, J., Guo, Q., Lin, L., Wang, Z., 2013. Progressive accretionary tectonics of the Beishan orogenic collage, Southern Altaids: insights from zircon U-Pb and Hf isotopic data of high-grade complexes. *Precambrian Research* 227, 368-388.
- Song, D., Xiao, W., Han, C., Tian, Z., 2013a. Geochronological and geochemical study of gneiss-schist complexes and associated granitoids, Beishan Orogen, southern Altaids. *International Geology Review* 55, 1705-1727.
- Song, D., Xiao, W., Han, C., Tian, Z., Wang, Z., 2013b. Provenance of metasedimentary rocks from the Beishan orogenic collage, southern Altaids: Constraints from detrital zircon U-Pb and Hf isotopic data. *Gondwana Research* 24, 1127-1151.
- Song, T.Z., Wang, J., Lin, H., Yang, X.F., Zhang, L., An, S.W., 2008. The Geological Features of Ophiolites of Xiaohuangshan in Beishan Area, Inner Mongolia. *Northwestern Geology* 41, 55-63 (in Chinese with English abstract).
- Steiger, R.H., Jäger, E., 1977. Subcommittee on geochronology: Convention on the use of decay constants in geo- and cosmochronology. *Earth and Planetary Science Letters* 36, 359-362.
- Stern, C.R., 2011. Subduction erosion: rates, mechanism, and its role in arc magmatism and the evolution of the continental crust. *Gondwana Research* 20, 284-308.
- Tian, Z., Xiao, W., Shan, Y., Windley, B., Han, C., Zhang, J.e., Song, D., 2013a. Mega-fold interference patterns in the Beishan orogen (NW China) created by

- change in plate configuration during Permo-Triassic termination of the Altaids. *Journal of Structural Geology* 52, 119-135.
- Tian, Z., Xiao, W., Windley, B.F., Lin, L.n., Han, C., Zhang, J.e., Wan, B., Ao, S., Song, D., Feng, J., 2013b. Structure, age, and tectonic development of the Huoshishan-Niujuanzi ophiolitic mélangé, Beishan, southernmost Altaids. *Gondwana Research* 25, 820-841.
- Wakita, K., Pubellier, M., Windley, B.F., 2013. Tectonic processes from rifting to collision via subduction in SE Asia and the western Pacific: A key to understanding the architecture of the Central Asian Orogenic Belt. *Lithosphere* 5, 265-278.
- Wan, B., Xiao, W., Windley, B.F., Yuan, C., 2013. Permian hornblende gabbros in the Chinese Altai from a subduction-related hydrous parent magma, not from the Tarim mantle plume. *Lithosphere* 5, 290-299.
- Wang, F., Zhou, X.-H., Zhang, L.-C., Ying, J.-F., Zhang, Y.-T., Wu, F.-Y., Zhu, R.-X., 2006. Late Mesozoic volcanism in the Great Xing'an Range (NE China): Timing and implications for the dynamic setting of NE Asia. *Earth and Planetary Science Letters* 251, 179-198.
- Wang, Y., Sun, G., Li, J., 2010. U-Pb (SHRIMP) and $^{40}\text{Ar}/^{39}\text{Ar}$ geochronological constraints on the evolution of the Xingxingxia shear zone, NW China: A Triassic segment of the Altyn Tagh fault system. *Geological Society of America Bulletin* 122, 487-505.
- Wilhem, C., Windley, B.F., Stampfli, G.M., 2012. The Altaids of Central Asia: A tectonic and evolutionary innovative review. *Earth-Science Reviews* 113, 303-341.
- Windley, B.F., Alexeiev, D., Xiao, W.J., Kroner, A., Badarch, G., 2007. Tectonic models for accretion of the Central Asian Orogenic Belt. *Journal of the Geological Society* 164, 31-47.
- Wu, F.Y., Yang, Y.H., Xie, L.W., Yang, J.H., Xu, P., 2006. Hf isotopic compositions of the standard zircons and baddeleyites used in U-Pb geochronology. *Chemical Geology* 234, 105-126.

- Xiao, W., Han, C., Liu, W., Wan, B., Zhang, J.e., Ao, S., Zhang, Z., Song, D., Tian, Z., Luo, J., 2014. How many sutures in the southern Central Asian Orogenic Belt: Insights from East Xinjiang-West Gansu (NW China)? *Geoscience Frontiers* 5, 525-536.
- Xiao, W., Santosh, M., 2014. The western Central Asian Orogenic Belt: A window to accretionary orogenesis and continental growth. *Gondwana Research* 25, 1429-1444.
- Xiao, W., Windley, B.F., Allen, M.B., Han, C., 2013. Paleozoic multiple accretionary and collisional tectonics of the Chinese Tianshan orogenic collage. *Gondwana Research* 23, 1316-1341.
- Xiao, W., Windley, B.F., Badarch, G., Sun, S., Li, J., Qin, K., Wang, Z., 2004. Palaeozoic accretionary and convergent tectonics of the southern Altaids: implications for the growth of Central Asia. *Journal of the Geological Society* 161, 339-342.
- Xiao, W.J., B. F. Windley, B. C. Huang, C. M. Han, C. Yuan, H. L. Chen, M. Sun, Sun, S., Li, J.L., 2009a. End-Permian to mid-Triassic termination of the accretionary processes of the southern Altaids: implications for the geodynamic evolution, Phanerozoic continental growth, and metallogeny of Central Asia. *International Journal of Earth Sciences*. 98, 1185–1188, doi: 10.1007/s00531-009-0418-4.
- Xiao, W.J., Mao, Q.G., Windley, B.F., Han, C.M., Qu, J.F., Zhang, J.E., Ao, S.J., Guo, Q.Q., Cleven, N.R., Lin, S.F., Shan, Y.H., Li, J.L., 2010. Paleozoic multiple accretionary and collisional processes of the Beishan orogenic collage. *American Journal of Science* 310, 1553-1594, doi: 10.2475/10.2010.12.
- Xiao, W.J., Windley, B.F., Hao, J., Zhai, M.G., 2003. Accretion leading to collision and the Permian Solonker suture, Inner Mongolia, China: Termination of the central Asian orogenic belt. *Tectonics* 22, 1069-1089, doi: 10.1029/2002TC001484.
- Xiao, W.J., Windley, B.F., Yuan, C., Sun, M., Han, C.M., Lin, S.F., Chen, H.L., Yan, Q.R., Liu, D.Y., Qin, K.Z., Li, J.L., Sun, S., 2009b. Paleozoic multiple subduction-accretion processes of the southern Altaids. *American Journal of Science* 309, 221-270.

- Xie, L.W., Zhang, Y.B., Zhang, H.H., Sun, J.F., Wu, F.Y., 2008. In situ simultaneous determination of trace elements, U-Pb and Lu-Hf isotopes in zircon and baddeleyite. *Chinese Science Bulletin* 53, 1565-1573.
- Xu, X.Y., He, H.P., Wang, H.L., Chen, J.L., 2009. Geological settings of the metallogeny of the Eastern Tian Shan and Beishan areas, 1:1,000,000: Beijing, China, Geological Publishing House.
- Yakubchuk, A., 2004. Architecture and mineral deposit settings of the Altaid orogenic collage: a revised model. *Journal of Asian Earth Sciences* 23, 761-779.
- Yang, L.K., Wang, F., Shen, J.L., Chen, R., Xing, G.F., 2008. Lasing on pyroclastic rocks: A case study of $^{40}\text{Ar}/^{39}\text{Ar}$ dating on Moshishan Group, eastern Zhejiang Province. *Chinese Science Bulletin* 53, 3876-3882.
- Zhang, J., Li, J., Liu, J., Li, Y., Qu, J., Feng, Q., 2012. The relationship between the Alxa block and the North China Plate during the Early Paleozoic: New information from the Middle Ordovician detrital zircon ages in the eastern Alxa block. *Acta Petrologica Sinica* (in Chinese with English abstract) 28, 2912-2934.
- Zhang, Y., Wang, Z., Yan, Z., Wang, T., Guo, X., 2011. Provenance of Neoproterozoic rocks in Quruqtagh area, Xinjinag: Evidence from detrital zircon geochronology. *Acta Petrologica Sinica* (in Chinese with English abstract) 27, 121-132.
- Zheng, R., Wu, T., Zhang, W., Xu, C., Meng, Q., 2013. Late Paleozoic subduction system in the southern Central Asian Orogenic Belt: Evidences from geochronology and geochemistry of the Xiaohuangshan ophiolite in the Beishan orogenic belt. *Journal of Asian Earth Sciences* 62, 463-475.
- Zhou, J.-B., Wilde, S.A., 2013. The crustal accretion history and tectonic evolution of the NE China segment of the Central Asian Orogenic Belt. *Gondwana Research* 23, 1365-1377.
- Zuo, G.C, Zhang, S., He, G., Zhang, Y., 1991. Plate tectonic characteristics during the early paleozoic in Beishan near the Sino-Mongolian border region, China. *Tectonophysics* 188, 385-392.

- Zuo, G.C, Zhang, S.L., He, G.Q., Zhang, Y., 1990a. Early Paleozoic plate tectonics in Beishan area. *Scientia Geologica Sinica* (in Chinese with English abstract), 4 , 305-314.
- Zuo, G.C., Liu, Y.K., Liu, C.Y., 2003. Framework and evolution of the tectonic structure in Beishan area across Gansu Province, Xinjiang Autonomous region and Inner Mongolia Autonomous Region. *Acta Geologica Gansu* (in Chinese with English abstract), 12, 1-15.
- Zuo, G.C., Zhang, S.L., Wang, X., Jin, S.Q., He, G.Q., Zhang, Y., Li, H.C., Bai, W.C., 1990b. Plate Tectonics and Metallogenic Regularities in Beishan Region, Peking University Publishing House, (in Chinese with English abstract).

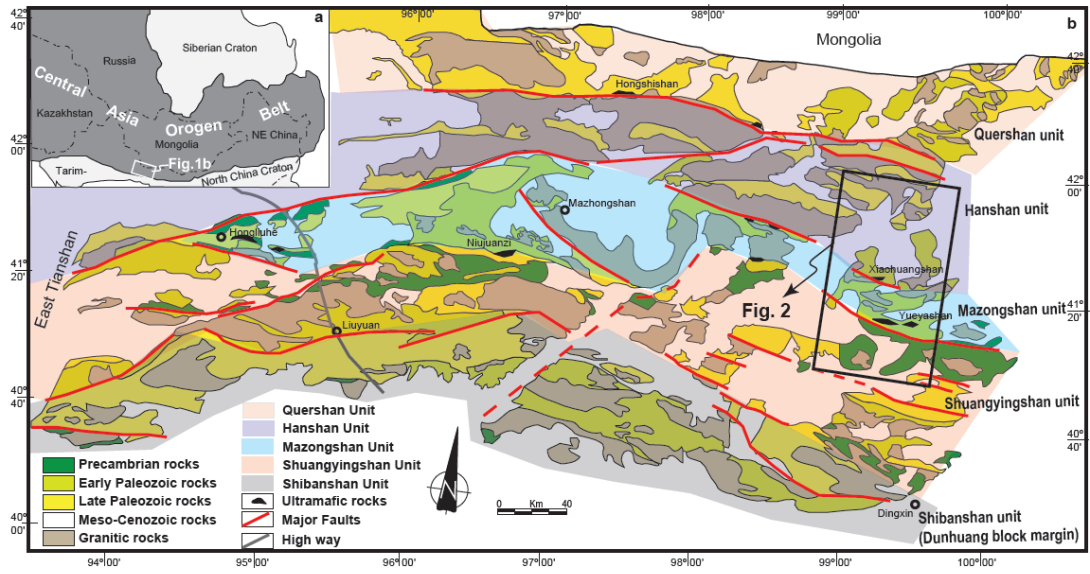


Figure 1

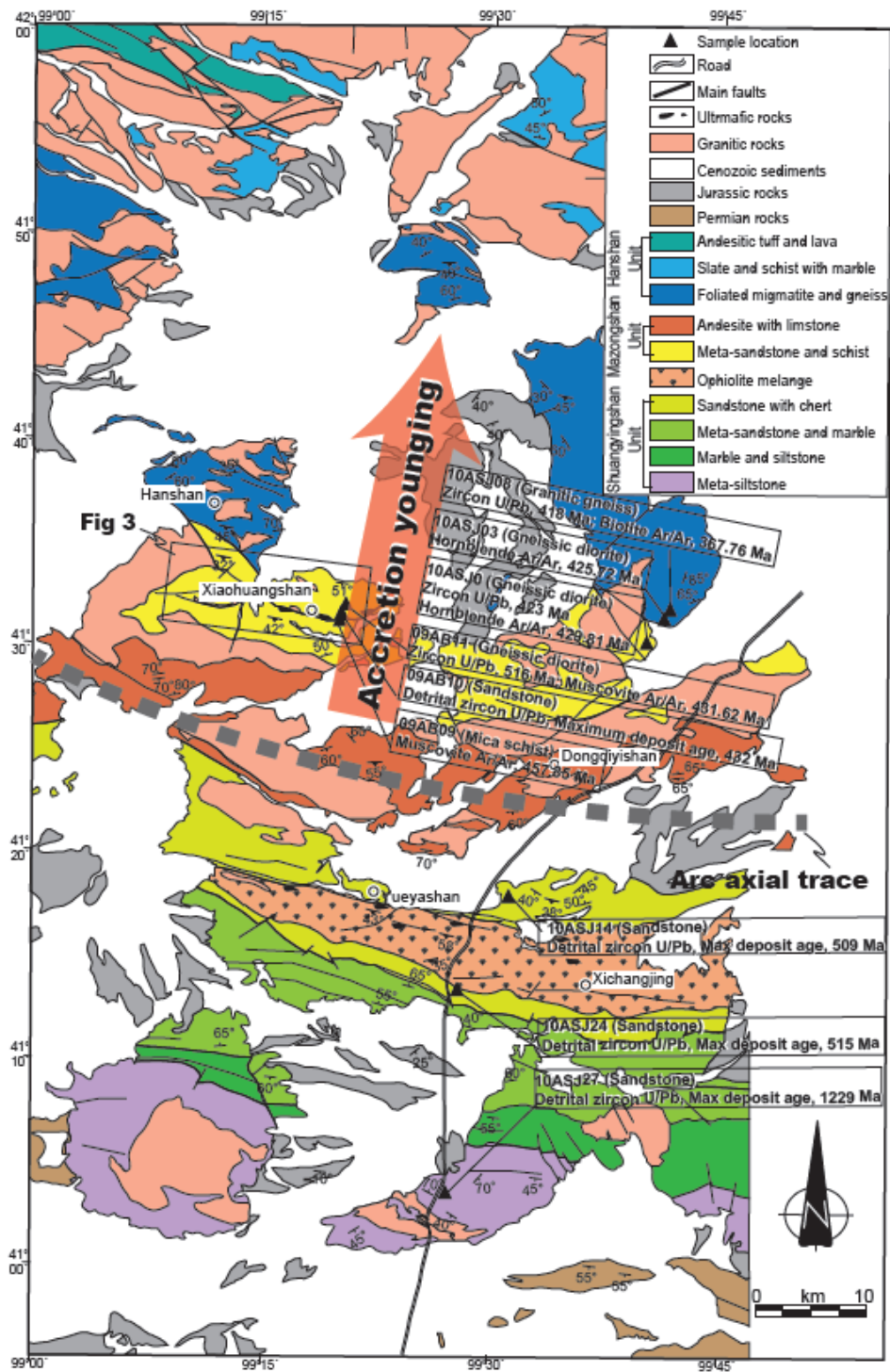


Figure 2

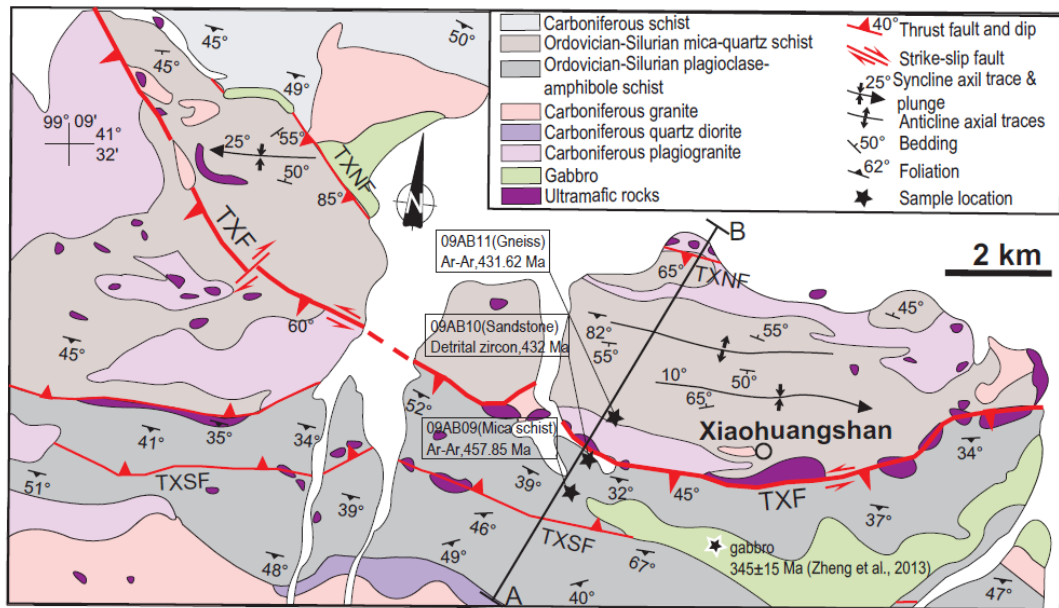


Fig. 3

ACCEPTED MANUSCRIPT

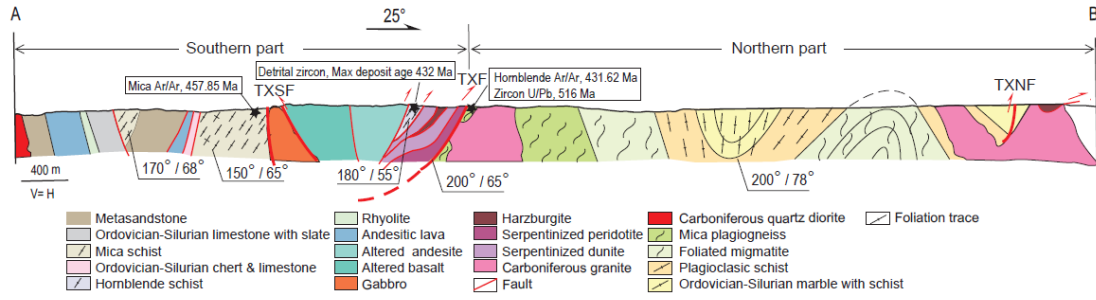


Fig. 4

ACCEPTED MANUSCRIPT

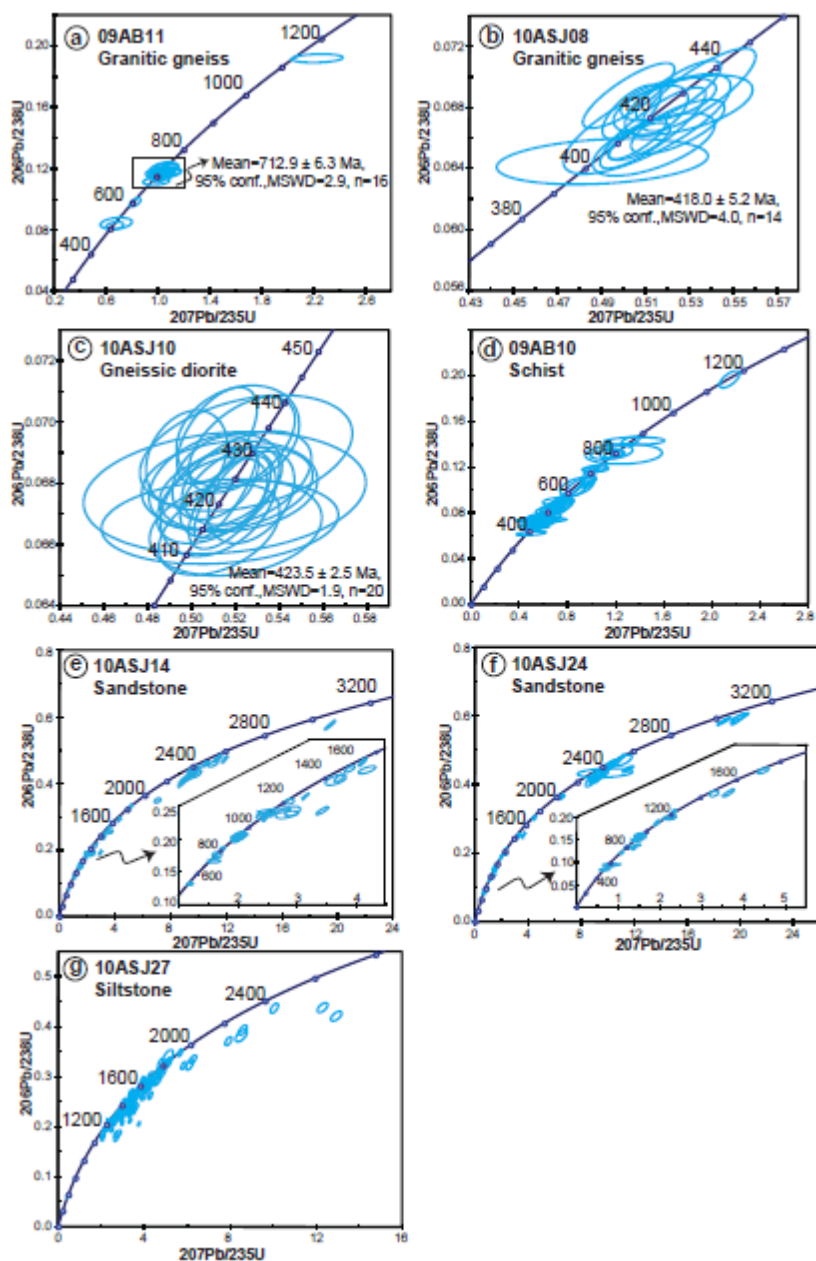


Figure 5

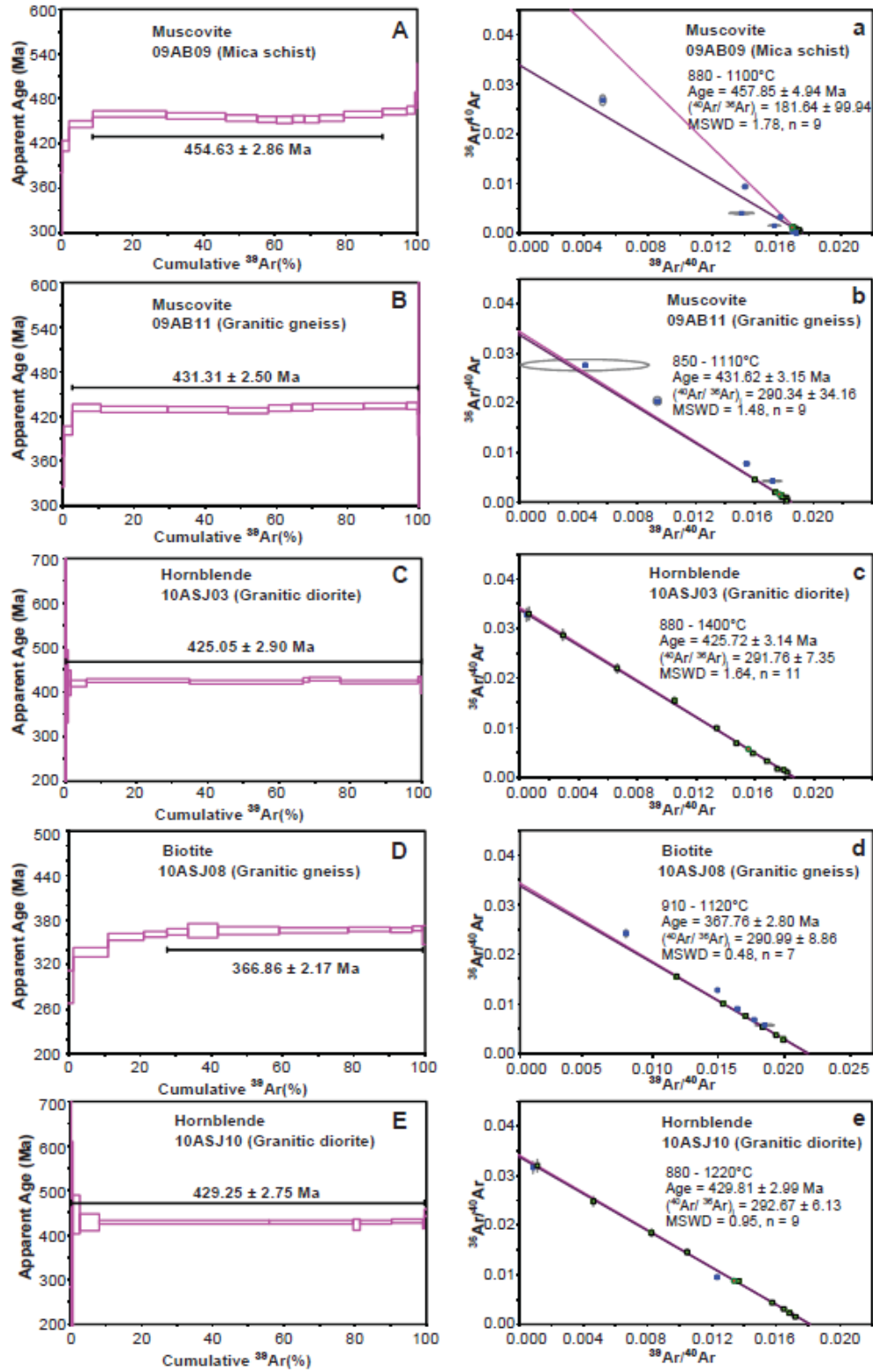


Figure 6

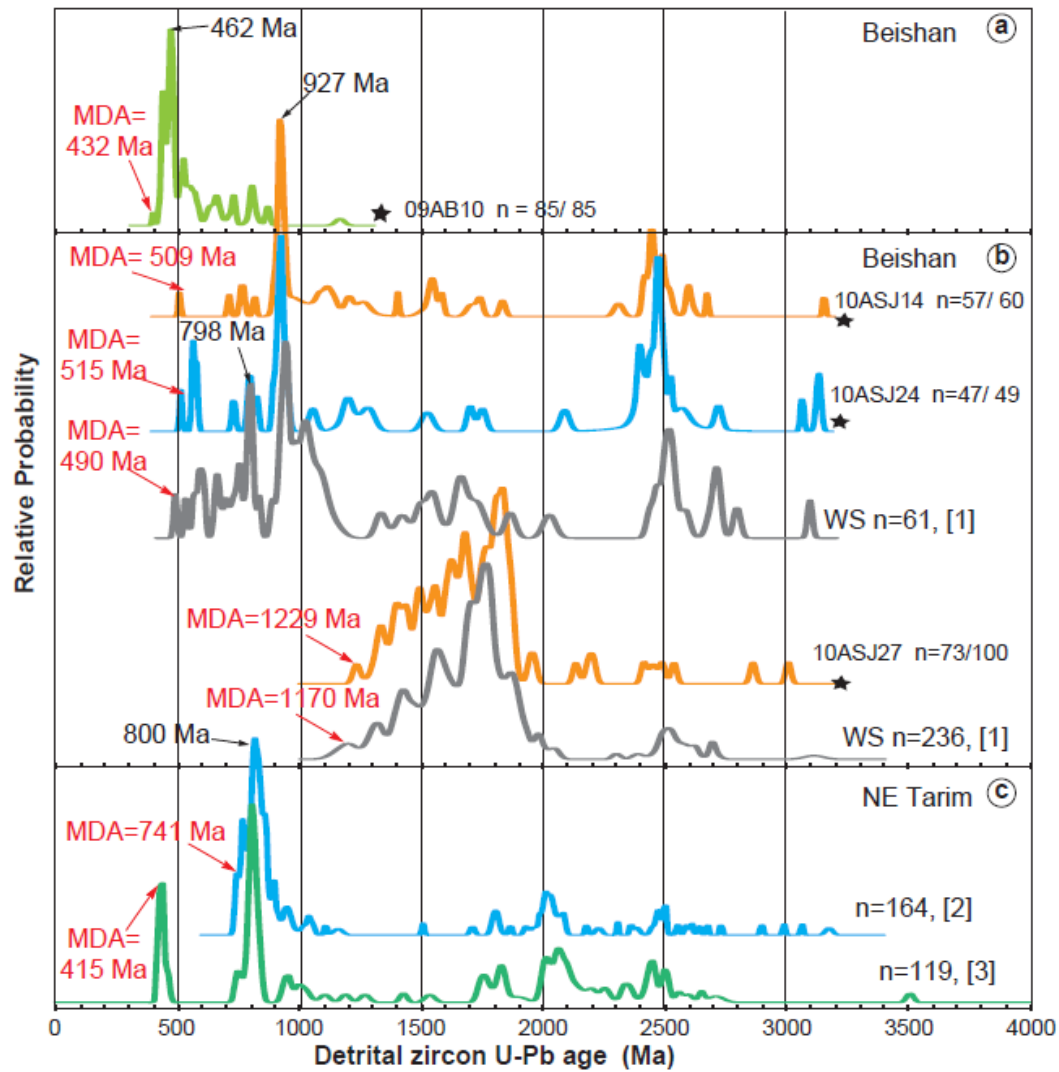


Fig. 7

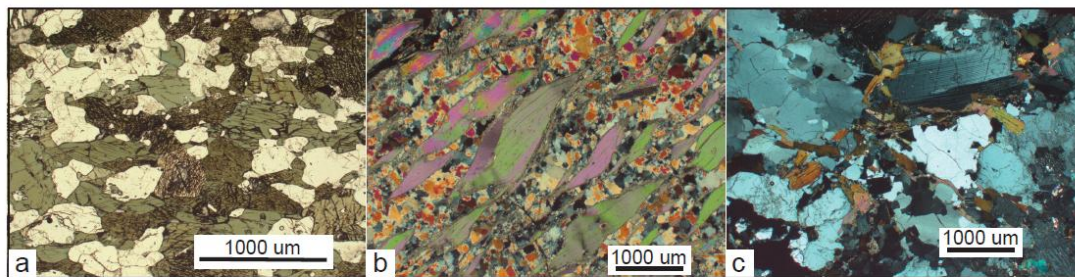


Fig. 8

ACCEPTED MANUSCRIPT

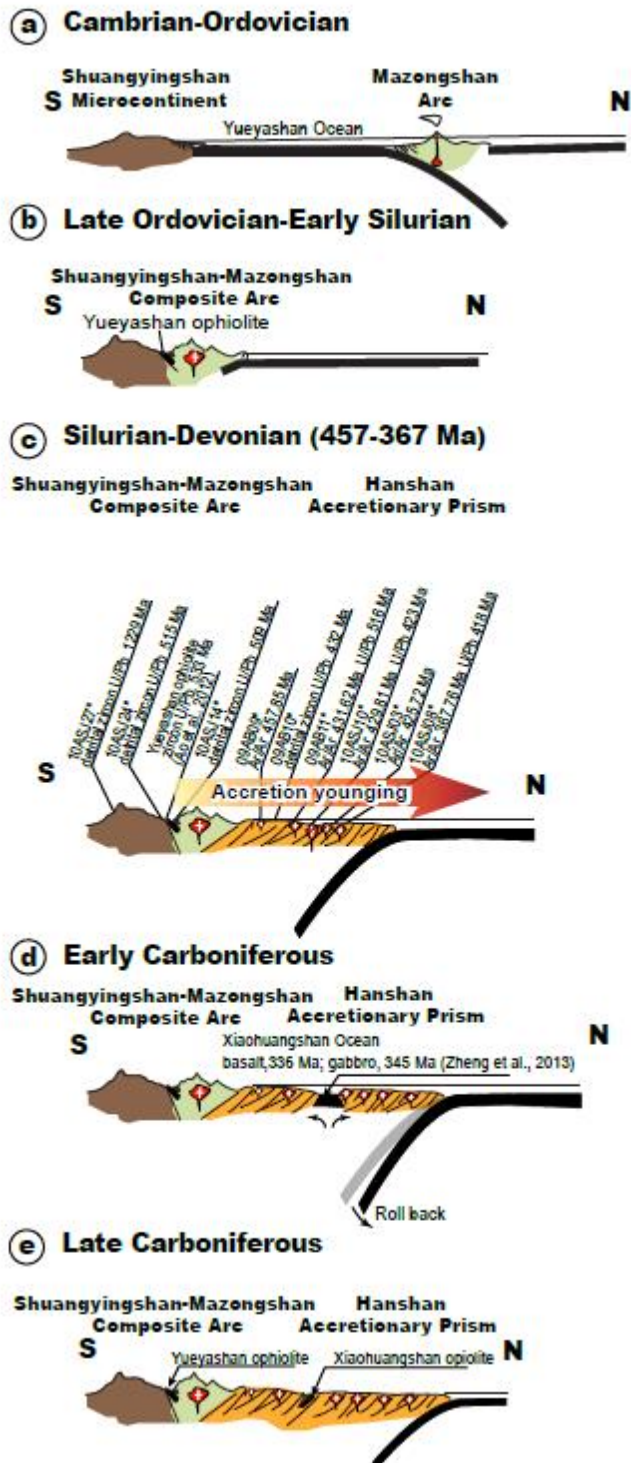
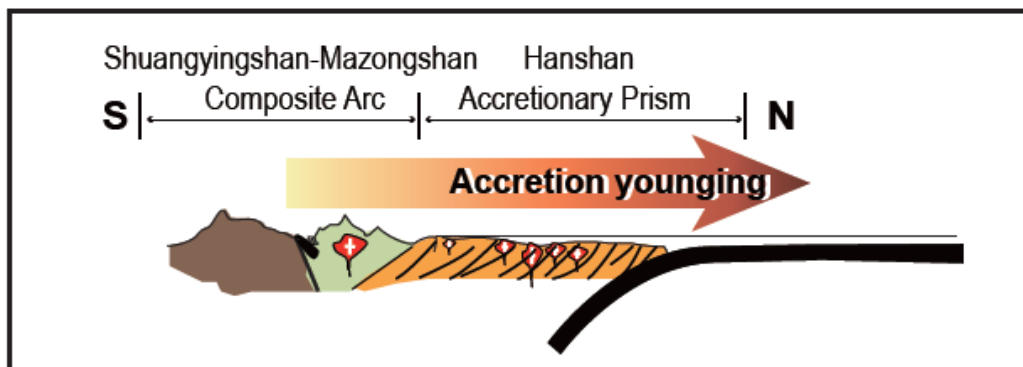


Figure 9



Graphical abstract

ACCEPTED MANUSCRIPT

Highlights

Shuangyingshan is a micro-continent, which shares age peaks with Tarim block before 741 Ma.

Hanshan is an accretionary prism, which accreted continuously from south to north.

Xiaohuangshan Ocean formed as an intra-arc basin within the forearc accretionary prism.